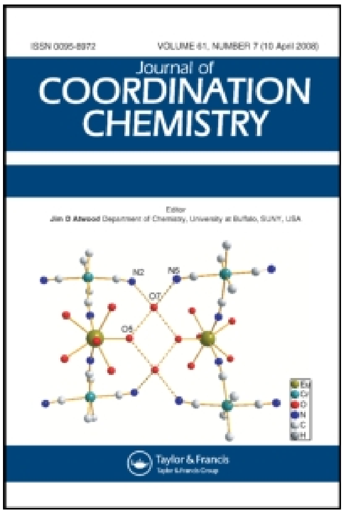

Journal of Coordination Chemistry
Publication details, including instructions for authors and subscription information:
http://www.informaworld.com/smpp/title~content=t713455674

A melamine-adipate-bridged binuclear copper complex with supramolecular architecture: synthesis, structures, and properties of $[Cu_2(MA)(ad)_2]\cdot H_2O$ and $(MA)\cdot(H_2ad)\cdot H_2O$

Hai-Yan Zhao[a]; Feng-Ying Bai[a]; Yong-Heng Xing[a]; Zhang-Peng Li[a]; Yun-Zhu Cao[a]; Xiao-Qing Zeng[b]; Mao-Fa Ge[b]
[a] College of Chemistry and Chemical Engineering, Liaoning Normal University, Dalia, 116029, P.R. China [b] Institute of Chemistry, Chinese Academy of Sciences, Beijing 100080, P.R. China

To cite this Article Zhao, Hai-Yan , Bai, Feng-Ying , Xing, Yong-Heng , Li, Zhang-Peng , Cao, Yun-Zhu , Zeng, Xiao-Qing and Ge, Mao-Fa(2010) 'A melamine-adipate-bridged binuclear copper complex with supramolecular architecture: synthesis, structures, and properties of $[Cu_2(MA)(ad)_2]\cdot H_2O$ and $(MA)\cdot(H_2ad)\cdot H_2O$', Journal of Coordination Chemistry, 63: 3, 435 — 447, First published on: 24 November 2009 (iFirst)

To link to this Article: DOI: 10.1080/00958970903437024

URL: http://dx.doi.org/10.1080/00958970903437024

Journal of Coordination Chemistry
Vol. 63, No. 3, 10 February 2010, 435–447

Taylor & Francis
Taylor & Francis Group

A melamine–adipate-bridged binuclear copper complex with supramolecular architecture: synthesis, structures, and properties of $[Cu_2(MA)(ad)_2] \cdot H_2O$ and $(MA) \cdot (H_2ad) \cdot H_2O$

HAI-YAN ZHAO†, FENG-YING BAI†, YONG-HENG XING*†,
ZHANG-PENG LI†, YUN-ZHU CAO†, XIAO-QING ZENG‡ and MAO-FA GE‡

†College of Chemistry and Chemical Engineering, Liaoning Normal University,
Huanghe Road 850#, Dalia, 116029, P.R. China
‡Institute of Chemistry, Chinese Academy of Sciences, Beijing 100080, P.R. China

(*Received 18 June 2009; in final form 14 August 2009*)

Complexes of melamine with adipic acid and $Cu(CH_3COO)_2 \cdot H_2O$, $[Cu_2(MA)(ad)_2] \cdot H_2O$ (**1**), and $(MA) \cdot (H_2ad) \cdot H_2O$ (**2**) (MA = melamine; H_2ad = adipic acid) have been synthesized under hydrothermal conditions and characterized by elemental analysis, infrared, UV-Vis, and single crystal X-ray diffraction. Both crystallized in the triclinic space group *P-1*. In **1**, MA and adipate bond to copper to construct a 3-D supramolecular framework in an unusual noninterpenetrated pseudo-primitive cubic topology constructed from a four-connected binuclear Cu(II) secondary building unit. A variety of intra- or inter-molecular hydrogen bonds exist. In **2**, the 3-D supramolecular structure is formed through strong interactions among MA, adipic acid, and lattice water. Thermal analysis, photoluminescence, and calculations were also performed.

Keywords: Melamine; Synthesis; Supramolecular complexes; Crystal structure; Hydrogen bonds

1. Introduction

Organo copper complexes have intriguing frameworks and potential application in adsorption [1], magnetism [2], nonlinear optical activity [3], catalysis [4], metalloenzymes [5], and many other fields [6]. Ligands are typically azide [7], amino acid [8], poly(pyrazolyl)borate [9], multicarboxylate [10], Schiff base [11], etc. Studies on copper–melamine (MA) coordination chemistry is in its infancy.

Melamine, first obtained by Liebig in 1834, contains three nitrogens as part of a six-member aromatic heterocycle and three amino groups at the three carbons of the cycle, enabling it to be an excellent hydrogen donor and acceptor with diverse hydrogen bonding and interesting architectures [12–17]. The three heterocyclic nitrogens can potentially coordinate to metal ions as high-spin secondary building unit (SBU) to construct metal–organic frameworks. Coordination chemistry of MA remains rarely

---

*Corresponding author. Email: yhxing2000@yahoo.com

Journal of Coordination Chemistry
ISSN 0095-8972 print/ISSN 1029-0389 online
DOI: 10.1080/00958970903437024

explored; however, several complexes are reported [18–31]. In these complexes, the MA either does not directly bond to metal [20–22, 31] or it affords only one ring N in coordination [20, 22–24, 29]. This may be due to: (1) the trend to form hydrogen bonds between MA molecules; (2) the space block between adjacent amine groups; (3) the strong rigidity of the N-heterocycle. Among the MA literatures, only a few copper complexes have been reported [19, 25, 26, 29] with monodentate MA. Carboxylates have been widely used in the build-up of supramolecular materials [32, 33] with diverse coordination, chelating to one metal center, and bridging bidentate in a syn–syn, syn–anti, or anti–anti configuration to two metal centers [34, 35].

In this article, we report the hydrothermal synthesis, crystal structures, and properties of the first copper–MA–adipate framework which contains four-connected binuclear Cu(II) SBUs and a supramolecular architecture: $[Cu_2(MA)(ad)_2]\cdot H_2O$ (**1**) and $(MA)\cdot(H_2ad)\cdot H_2O$ (**2**). Their hydrogen bonds are discussed in detail.

2. Experimental

2.1. *Reagents and instruments*

All chemicals were of analytical grade and used without purification. Elemental analyses were performed on a Perkin-Elmer 240C automatic analyzer. The infrared (IR) spectra were recorded on a JASCO FT/IR-480 PLUS Fourier Transform spectrophotometer with pressed KBr pellets from 200 to 4000 cm^{-1}; UV-Vis spectra were obtained on a JASCO V-570 UV-Vis spectrometer (200–1100 nm as solids). The luminescence spectra were reported on a JASCO FP-6500 spectrofluorimeter (solid) in the range of 200–850 nm. X-ray powder diffraction (XRD) data were collected on a Bruker Advance-D8 with Cu-Kα radiation in the range $5^\circ < 2\theta < 60^\circ$, with a step size of $0.02^\circ(2\theta)$ and an acquisition time of 2 s per step.

2.2. *Preparation of 1 and 2*

2.2.1. Preparation of $[Cu_2(MA)(ad)_2]\cdot H_2O$ (1). Compound **1** was prepared by a hydrothermal reaction. A mixture of adipic acid (0.22 g, 1.5 mmol), MA (0.12 g, 1 mmol), and H_2O (10 mL) was sealed into a bomb equipped with a Teflon liner, heated at 120°C for 2 days, then $Cu(CH_3COO)_2\cdot H_2O$ (0.19 g, 0.1 mmol) in H_2O (2 mL) was added and the mixture was heated at 120°C for another 2 days, then cooled at 10°C for 3 h to 100°C, followed by slow cooling to room temperature. Deep-blue block crystals for **1** were obtained. Yield: 0.21 g, 79.26% (based on Cu). Anal. Calcd for $C_{15}H_{24}N_6O_9Cu_2$ (%): C, 32.30; H, 4.32; N, 15.02. Found (%): C, 32.36; H, 4.28; N, 15.13. IR (KBr, ν, cm^{-1}): 3455, 3410, 3377, 3231, 2915, 2861, 2680, 1648, 1616, 1547, 1442, 1423, 1317, 1177, 852, 808, 762, 688, 641, 610, 447, 368. UV-Vis (λ_{max}, nm): 258, 308, 388.

2.2.2. Preparation of $(MA)\cdot(H_2ad)\cdot H_2O$ (2). Compound **2** was synthesized by a method similar to that of **1**. A mixture of adipic acid (0.22 g, 1.5 mmol), MA (0.12 g, 1 mmol), and H_2O (12 mL) was sealed into a bomb equipped with a Teflon liner, heated at 120°C for 5 days, and then cooled at 10°C for 3 h to 100°C, followed by slow cooling to room temperature. Some colorless crystals suitable for X-ray were obtained. Yield: 0.17 g, 60.24% (based on MA). Anal. Calcd for $C_9H_{18}N_6O_5$ (%): C, 37.24; H, 6.25; N, 28.95. Found (%): C, 37.13; H, 6.32; N, 28.82. IR (KBr, ν, cm^{-1}): 3354, 3223, 3091, 2934, 2867, 2694, 1681, 1660, 1525, 1498, 1422, 1326, 1273, 1156, 1110, 1050, 926, 784, 761, 687, 651, 582. UV-Vis (λ_{max}, nm): 246, 294, 362.

2.3. *X-ray data collection and refinement of crystal structures*

Crystals of **1** and **2** were mounted on glass fibers for X-ray measurement. Reflection data were collected at room temperature on a Bruker AXS SMART APEX II CCD diffractometer with graphite-monochromated Mo-Kα radiation ($\lambda = 0.71073$) and $\omega - 2\theta$ scan mode. All measured independent reflections were used in the structural analyses and semi-empirical absorption corrections were applied using SADABS [36].

The structures were solved by direct methods using SHELXS-86 and refined using SHELXL-97 [37]. All hydrogens were positioned geometrically and refined using a riding model. The nonhydrogen atoms were refined with anisotropic thermal parameters. Crystallographic data and experimental details of the data collection and the structure refinement are given in table 1. Drawings were made with the Diamond program.

Table 1. Crystallographic data and structure refinement for **1** and **2**.

Empirical formula	$C_{15}H_{24}N_6O_9Cu_2$	$C_9H_{18}N_6O_5$
Formula weight ($g\,mol^{-1}$)	559.48	290.29
Crystal system	Triclinic	Triclinic
Space group	*P*-1	*P*-1
Unit cell dimensions (Å, °)		
a	8.5396(17)	4.7211(9)
b	8.8775(18)	9.6404(19)
c	15.661(3)	15.596(3)
α	77.24(3)	105.14(3)
β	83.36(3)	92.77(3)
γ	64.96(3)	99.29(3)
Volume (Å^3), *Z*	1048.8(4), 2	673.1(2), 2
Calculated density ($g\,cm^{-3}$)	1.772	1.432
Crystal size (mm^3)	0.12 × 0.10 × 0.09	0.15 × 0.13 × 0.08
F(000)	572	308
μ(Mo-Kα) (cm^{-1})	20.90	1.17
θ range for data collection (°)	3.12–27.48	3.10–27.47
Reflections collected	10308	6663
Independent reflections [$I > 2\sigma(I)$]	4753	3048
Parameters	297	237
Largest difference peak and hole (e Å^{-3})	0.532, −0.352	0.629, −0.288
Goodness-of-fit	1.148	1.036
R^a	$0.0281(0.0356)^b$	$0.0462(0.0625)^b$
$wR_2{}^a$	$0.0779(0.0936)^b$	$0.1451(0.1558)^b$

[a] $R = \Sigma||F_o|-|F_c||/\Sigma|F_o|$, $wR_2 = \{\Sigma[w(F_o^2 - F_c^2)^2]/\Sigma[w(F_o^2)^2]\}^{1/2}$; $[F_o > 4\sigma(F_o)]$.

[b] Based on all data.

2.4. *Methods of quantum chemistry calculation*

MP2 calculations at 6−31G* basis set level were carried out for the complexes with Gaussian 03W. The calculation included 161 and 58 atoms; 1430 and 506 basis functions; 2878 and 952 primitive Gaussians for **1** and **2**, respectively. The parameters of the molecular structures come from the crystal structure data, and the molecular point groups and their symmetry (C_s) are also considered. The electronic structures and the bonding of the complexes were analyzed with *ab initio* calculations and natural bonding orbital (NBO) analysis. The results of calculation give the constitution and the energy of the molecular orbital, NBO atomic charge.

2.5. *Thermogravimetric assay of 1*

Thermogravimetric analyses (TGA) for **1** was carried out on a Cahn Thermax 500 thermogravimetric/differential thermal analyzer instrument. The samples were initially heated for 1 h at 50°C to remove the rudimental air. During the simple ramping experiment, weight changes were recorded as a function of temperature for $10^{\circ}C\,min^{-1}$, temperature gradient between 50°C and 900°C in argon. The mass of **1** is 12.34 mg.

3. Results and discussion

3.1. *Synthesis*

By hydrothermal method, we have obtained $[Cu_2(MA)(ad)_2]\cdot H_2O$ (**1**) and $(MA)\cdot(H_2ad)\cdot H_2O$ (**2**) at 120°C in water. Systematic experiments have been carried out for different solvents (e.g., mixed solution of water–methanol, water–ethanol, and water–DMF), different mole ratios of MA and adipic acid, and different starting materials [e.g., $Cu(NO_3)_2$ and $CuCl_2$] to find their optimum reaction conditions. It is found that: (1) the final desired products can be obtained only in water or water–methanol solution, but can easily be reproduced in high yields in water; (2) the final product was the same, no matter the mole ratios of MA and adipic acid were 1 : 1.5 or 1 : 3; (3)when $Cu(NO_3)_2$ and $CuCl_2$ were used as a copper source, the product could not be obtained. In addition, the two complexes are quite stable in the solid state at room temperature and insoluble in DMF, DMSO, H_2O, MeOH, CH_2Cl_2, etc.

3.2. *Spectra properties*

3.2.1. IR spectra. The IR spectra of **1** and **2** are consistent with the structural data presented in this article. The spectra have bands at 3455–2680 cm^{-1} for **1** assigned to N–H and O–H stretches. Similarly, bands at 3354–2694 cm^{-1} for **2** are assigned to N–H and O–H stretches. The strong bands at 1616 cm^{-1} for **1** and 1660 cm^{-1} for **2** are attributed to C=N stretch from the MA. Bands at 1648 and 1442 cm^{-1} for **1**, and 1681 and 1422 cm^{-1} for **2** are assigned to asymmetric and symmetric stretches of the carboxyl from adipic acid. Bands in the range 1612–1498 cm^{-1} and 784–641 cm^{-1} for **1** and **2** are assigned to C=C of aromatic and C–H aromatic stretching vibrations. Bands at 1177 and 1156 cm^{-1} are due to C–N stretches. The Cu–O$_{(carboxyl)}$ and Cu–N absorptions at 447 and 368 cm^{-1} for **1** substantiate MA and adipate directly bonded to copper in **1**.

Comparison of the FT-IR spectra of MA and adipic acid, **1**, and **2** (figure S1) show differences between the substrates and products for their characteristic vibrations: (1) for the $\nu_{as}(COO^-)$ vibrations of adipic acid, **1**, and **2**, bands are observed with maxima at *ca* 1697, 1648 and 1681 cm^{-1} with obvious red shifts in **1** and **2**. (2) Similarly, for the C=N stretching vibrations of MA, **1**, and **2**, bands are observed with maxima at 1652, 1616, and 1660 cm^{-1} showing a red shift in **1** and a blue shift in **2**.

3.2.2. UV-Vis absorption spectra.

The UV-Vis absorption spectra of **1** and **2** as solids show sharp and strong high-energy absorptions at 258 and 308 nm for **1** and 246 and 294 nm for **2** assigned as π–π* transitions of the aromatic-like chromophore from MA or adipic acid. A band at 394 nm for **1** is attributed to charge transitions of MA to metal (LMCT). A band at 362 nm for **2** is assigned as *n*–π* transition from MA and adipic acid.

A comparison of UV-Vis absorption spectra of the two compounds shows that red shift was found in the UV-Vis absorption spectra of **1** due to the coordination of MA and adipate.

3.3. *Structural description*

The molecular structures of $[Cu_2(MA)(ad)_2] \cdot H_2O$ (**1**) and $(MA) \cdot (H_2ad) \cdot H_2O$ (**2**) with the atom-numbering scheme are depicted in figures 1 and S2, respectively. The principal bond lengths are listed in tables 2 and 3 and angles in tables S1 and S2. Both compounds contain MA and adipic acid. In addition, there are abundant inter- and intra-molecular hydrogen bonds (table 4).

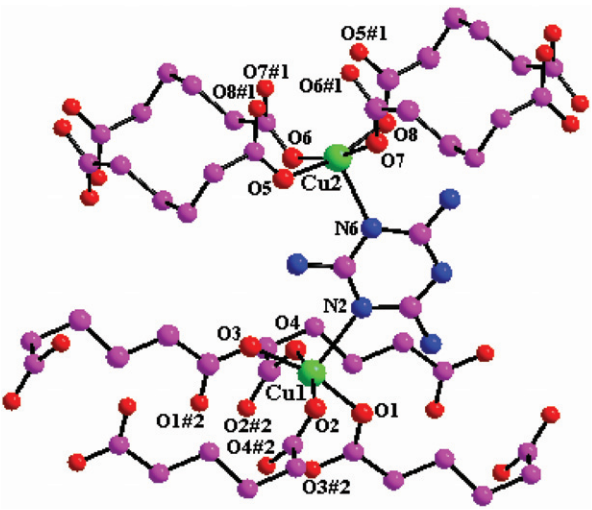

Figure 1. The molecular structure of **1**. (The lattice water molecule and all H atoms are omitted for clarity) (#1 : $2-x$, $1-y$, $2-z$; #2 : $1-x$, $2-y$, $1-z$).

Table 2. Selected bond lengths (Å) for **1**.

Cu1–O1	1.973(2)	C1–N1	1.335(4)	C2–N4	1.343(3)
Cu1–O2	1.961(2)	C2–N3	1.329(4)	C3–N5	1.338(3)
Cu1–O3	1.967(2)	C3–N4	1.330(3)	C1–N6	1.349(3)
Cu1–O4	1.950(2)	C2–N2	1.354(3)	C1–N2	1.345(3)
Cu1–N2	2.356(2)	C4–O3	1.252(3)	C10–O5$^{\#1}$	1.261(3)
Cu2–O5	1.969(2)	C8–O4	1.261(3)	C13–O6$^{\#1}$	1.261(3)
Cu2–O6	1.986(2)	C13–O7	1.250(3)	C3–N6	1.354(3)
Cu2–O7	1.979(2)	C10–O8	1.252(3)	C4–O1$^{\#2}$	1.247(3)
Cu2–O8	1.960(2)	Cu2–N6	2.228(2)	C8–O2$^{\#2}$	1.253(3)

Symmetry transformation used to generate equivalent atoms: #1: $2-x$, $1-y$, $2-z$; #2: $1-x$, $2-y$, $1-z$.

Table 3. Selected bond lengths (Å) for **2**.

C1–N1	1.310(2)	C2–N4	1.371(2)	C4–O1	1.203(2)
C1–N2	1.353(2)	C3–N5	1.318(2)	C4–O2	1.308(2)
C1–N6	1.359(2)	C3–N6	1.320(2)	C7–O4	1.252(2)
C2–N3	1.311(2)	C3–N4	1.357(2)	C7–O3	1.257(2)
C2–N2	1.321(2)				

Table 4. Hydrogen bonds of **1** and **2**.

D–H···A	*d*(D–H) (Å)	*d*(H···A) (Å)	*d*(D···A) (Å)	D–H–A (°)
Proposed hydrogen bonds for **1**				
O1W–H1WA···O6^{a}	0.783(0)	2.340(0)	3.100(7)	164.1(9)
O1W–H1WB···O4^{a}	0.793(5)	2.358(6)	3.108(8)	158.0(6)
N5–H5A···O1W^{b}	0.860(1)	2.155(1)	2.988(5)	162.9(4)
N1–H1A···O3	0.859(7)	1.883(8)	2.729(4)	167.2(0)
N1–H1B···O5	0.859(9)	2.009(7)	2.826(4)	158.2(4)
N3–H3B···O1	0.860(9)	1.926(3)	2.769(4)	165.7(7)
Proposed hydrogen bonds for **2**				
N3–H3A···N2^{a}	0.847(0)	2.182(0)	3.023(7)	172.4(1)
N1–H1A···O1W^{a}	0.860(0)	2.057(7)	2.864(9)	156.0(3)
N5–H5B···N6^{c}	0.876(0)	2.069(6)	2.943(4)	175.2(1)
N1–H1B···O1^{d}	0.860(0)	2.142(7)	2.989(8)	168.2(2)
O2–H2···O4^{e}	0.817(7)	1.799(9)	2.610(0)	170.6(1)
O1W–H1WB···O3^{f}	0.823(4)	2.103(0)	2.908(1)	165.7(4)
O1W–H1WA···O3	0.859(6)	1.903(3)	2.742(1)	164.8(0)
N3–H3B···O3	0.864(7)	2.003(2)	2.852(2)	166.9(3)
O4–H4···N4	1.082(6)	1.696(2)	2.763(6)	167.6(8)

Symmetry transformation used to generate equivalent atoms: a = $1-x$, $1-y$, $1-z$; b = $2-x$, $1-y$, $1-z$; c = $-1-x$, $-y$, $1-z$; d = $-x$, $1-y$, $1-z$; e = $1+x$, $1+y$, z; f = $1+x$, y, z.

X-ray crystallography reveals that, in **1** (figure 1), each copper atom is five-coordinated with one nitrogen from MA and four oxygens from different adipate groups. The MA ligand is coordinated to two coppers by ring nitrogens, while one adipate is coordinated to four coppers by four different oxygens. The structure of **1** can be evaluated by the Addision distortion index $\tau : \tau = |\beta - \alpha|/60^\circ$ [38], α and β being the two largest angles around the central atom. In a pentacoordinated system, values for τ in ideal polyhedra are 1.0 for trigonal bipyramidal and 0.0 for square pyramidal.

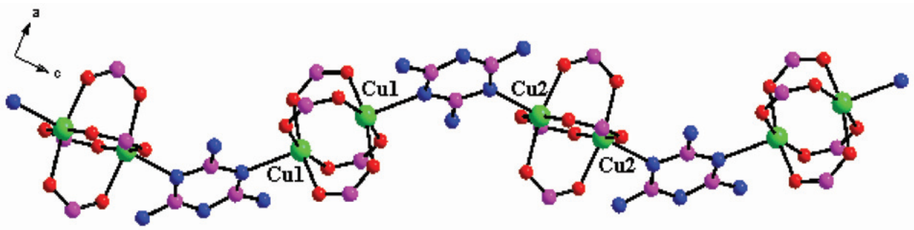

Figure 2. The 1-D chain structure of **1**. (All C and O atoms of adipate except for coordination carboxylates are omitted for clarity).

The value of τ is 0.07, indicating that the coordination environment of Cu is almost ideal square pyramidal. The deviations of O1, O2, O3, and O4 that compose the least-squares plane are −0.0072, 0.0073, −0.0075, and 0.0074 Å, respectively, showing that these atoms are on one plane. The Cu1 and N2 from the apical position lay 0.2487 and 2.5962 Å out of the O1–O2–O3–O4 coordination plane, indicating that Cu1 moves towards N2. Similarly, deviations of O5, O6, O7, and O8 composing another least-squares plane are −0.0006, 0.0006, 0.0006, and −0.0006 Å. Cu2 and N6 from the apical position lay −0.2248 and −2.4503 Å out of the O5–O6–O7–O8 coordination plane. The O–Cu–O bond angles range from 86.9(9)° to 166.9(8)° with the O–Cu distances from 2.026(8) to 2.299(3) Å; the N–Cu–O bond angles range from 92.1(9)° to 102.0(8)° with N–Cu distance from 2.228(2) to 2.356(2) Å, which is quite long due to Jahn–Teller effect. This Cu–N bond length is shorter than that found in $[Cu(HBA)_2(MA)_2]\cdot[Cu(HBA)_2]$ [2.573(9) Å] (HBA = 2-hydroxybenzaldehyde) [29], longer than those of $[Cu(C_3H_6N_6)(\mu\text{-}OCH_3)(ONO_2)(HOCH_3)]_2$ [2.010(2) Å] [19], $Cu_2Cl_2(\mu\text{-}Cl)(\mu\text{-}OCH_3)(CH_3OH)_2(MA)_2\cdot 2Et_2O$ [2.069(9), 2.077(1) Å], and $[Cu(\eta^1\text{-}OAc)(\mu\text{-}OCH_3)(MA)]_2\cdot 0.33H_2O$ [1.986(3) Å] [25].

If the binuclear Cu cluster is a single node located in the center of the cluster, this SBU ($Cu_2N_2O_4$) becomes a four-connected node. Each SBU is connected to the adjacent ones through MA ligands, forming a 1-D zigzag chain (figure 2). Adjacent chains are interlinked through two adipates, which coordinate to Cu1, forming a 2-D sheet (figure 3). Then, the 2-D sheets are connected by adipates which coordinated to Cu2, giving rise to the final 3-D framework (figure S3a). Therefore, each SBU connects to four adjacent SBUs, making the whole structure a pseudo-primitive cubic (pcu) metal–organic architecture, with partly double bonds between two nodes (figure S3b). Although many complexes with pcu topology have been reported, they contain only one kind of edges (all single or all double). However, this unusual four-connected SBU makes the present pcu contain both single and double edges. In addition, the nonbonded Cu···Cu separation in the SBU ($Cu_2N_2O_4$) is 2.667(50)–2.714(45) Å, which is close to $[Cu_2(OAc)_4(MA)(H_2O)]_2[Cu(HPE)_2]$ [2.678(2) Å] [HPE = 1-(2-hydroxyphenyl)ethanone] [29], and shorter than those of other Cu(II)–MA complexes [Cu···Cu = 3.0016(8)–3.171 Å] [19, 25].

In **1**, there are two kinds of hydrogen bonds (O–H···O and N–H···O) among the lattice water, adipate, and MA molecules, as is shown in figure 4, which contains intermolecular hydrogen bonds of O1W–H1WA···O6^a [3.100(7) Å, 164.1(9)°], O1W–H1WB···O4^a [3.108(8) Å, 158.0(6)°], N5–H5A···O1W^b [2.988 (5) Å, 162.9(4)°] ($a = 1 - x,\ 1 - y,\ 1 - z$; $b = 2 - x,\ 1 - y,\ 1 - z$) and other intramolecular hydrogen bonds between the amine groups and the carboxylate groups.

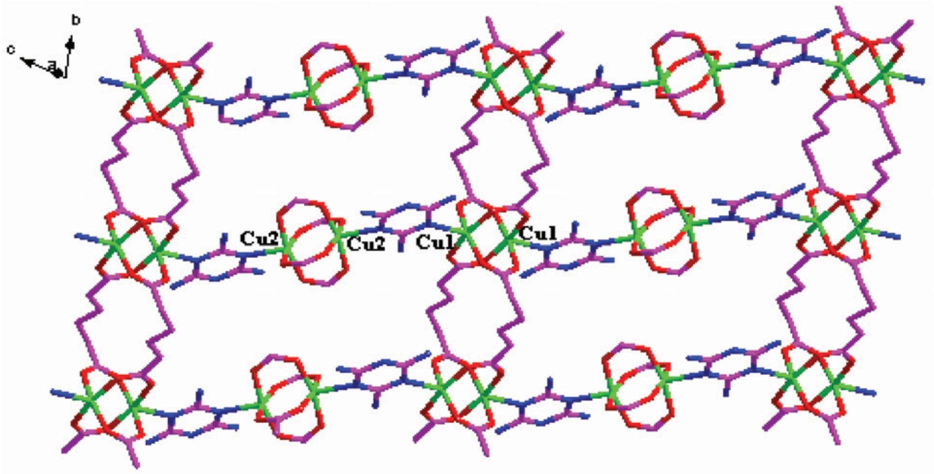

Figure 3. The 2-D layer structure of **1**.

For **2**, there is one MA, one water, and one adipic acid in an asymmetric unit. The MA molecules of **2** are interlinked through a pair of N–H$\cdots$N self-complementary hydrogen bonds with a $R_2^2(8)$ mode [N3–H3A$\cdots$N2^a, 3.023(7) Å, 172.4(1)° and N5–H5B$\cdots$N6^c, 2.943(4) Å, 175.2(1)°], forming the 1-D ribbon chain (figure 5). The adjacent chains are connected via hydrogen bonds of $R_3^3(10)$ [O1W–H1WA$\cdots$O3, 2.742(1) Å; N1–H1A$\cdots$O1W^a, 2.864(9) Å; N3–H3A$\cdots$N2^a, 3.023(7) Å and N3–H3B$\cdots$O3, 2.852(2) Å], $R_2^2(8)$ [N3–H3B$\cdots$O3, 2.852(2) Å and O4–H4$\cdots$N4, 2.763(6) Å], $R_4^4(14)$ [O2–H2$\cdots$O4^e, 2.610(0) Å; O4–H4$\cdots$N4, 2.763(6) Å; N5–H5B$\cdots$N6^c, 2.943(4) Å and N1–H1B$\cdots$O1^d, 2.989(8) Å] ($a = 1-x, 1-y, 1-z$; $b = 2-x, 1-y, 1-z$; $c = -1-x, -y, 1-z$; $d = -x, 1-y, 1-z$; $e = 1+x, 1+y, z$) motifs to generate a 2-D layer supramolecular structure [23, 29]; the final 3-D framework is obtained through the hydrogen bond of O1W–H1WB$\cdots$O3^f [2.908(1) Å, 165.7(4)°, $f = 1+x, y, z$] (figures S4 and S5).

Comparison of bond lengths and angles between the two compounds shows that the C–N$_{\text{amine}}$ bond lengths in **1** are longer than **2**, the orders of the internal C–N–C angles of the MA ring are **1** < **2**, and the order of the O–C–O angles in the carboxylate groups is **1** > **2**. Other corresponding bond lengths and angles between them are similar.

3.4. *Quantum chemistry calculations of 1 and 2*

According to molecular orbital theory, the frontiers orbitals and nearby molecular orbitals are important factors to stability. The larger the difference between the frontier orbitals, the more stable the molecular structure. The frontier molecular orbital symmetry and eigenvalues in Hartree for **1** and **2** show the highest occupied molecular orbitals (HOMO): –0.27665 and –0.35979 a.u. and the lowest unoccupied molecular orbital (LUMO): 0.08584 and 0.16816 a.u. The energy values of ΔE ($\Delta E = E_{\text{LUMO}} - E_{\text{HOMO}}$) for **1** and **2** are 0.36249 and 0.52795 a.u., respectively, and the corresponding chemical hardness is 0.18125 and 0.26398, respectively, showing the kinetic stability is **1** < **2** [39–41].

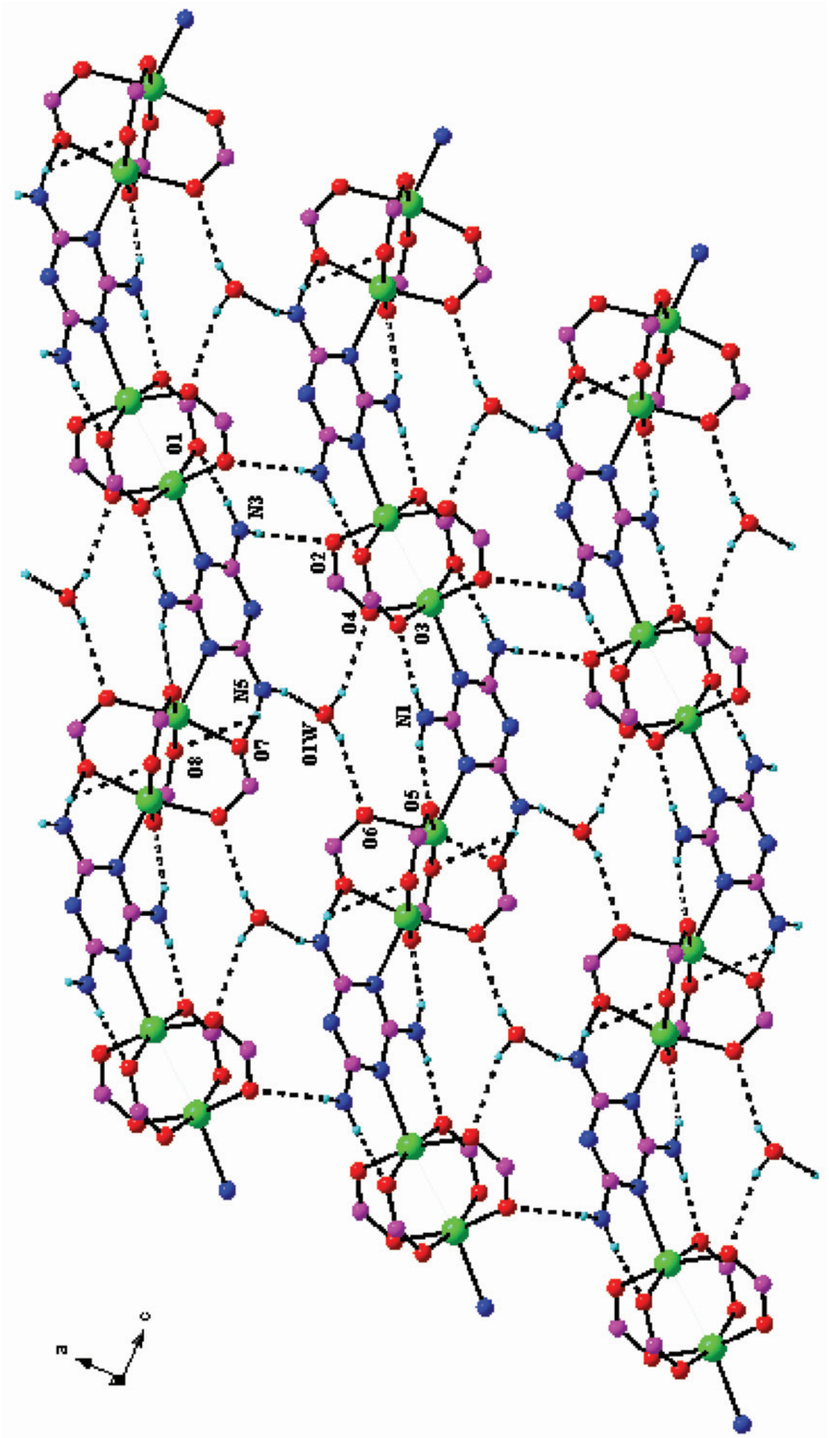

Figure 4. The connectivity of hydrogen bonds for **1**.

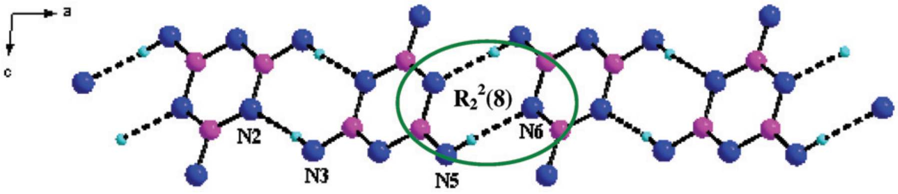

Figure 5. The 1-D ribbon chain through hydrogen bonds with a R_2^2 (8) mode in **2**.

Table 5. Selected Wiberg bond index and NBO bond order for **1**.

Bond	Cu1–O1	Cu1–O2	Cu1–O3	Cu1–O4	Cu1–N2
Wiberg bond index	0.2535	0.3328	0.3412	0.3104	0.0601
NBO bond order	0.1439	0.1628	0.1617	0.1560	0.0677
Bond	Cu2–O5	Cu2–O6	Cu2–O7	Cu2–O8	Cu2–N6
Wiberg bond index	0.2773	0.3994	0.2208	0.3367	0.0623
NBO bond order	0.1506	0.1693	0.1351	0.1619	0.0680

Some selected Wiberg bond indices and NBO bond orders for **1** are shown in table 5. The value of the bond order for Cu–O is in the range of 0.1351–0.1693 and for Cu–N is in the range of 0.0677–0.0680. Comparing the bond orders for them, Cu–N is smaller than Cu–O, consistent with the conclusion that the shorter the bond length, the larger the bond order leading to the stronger the bond. This result is consistent with the results of the crystallographic data of complex.

The atomic net charges and electron configurations for the complexes are shown in tables S3 and S4. The net charges of copper in **1** are 1.90367e and 1.90847e, showing that copper obtains some electrons from the ligands. For **1**, the net charges of coordinated oxygens range from −0.91033e to −0.83186e and for coordinated nitrogen from −0.90185e to −0.88739e; net charges of uncoordinated nitrogens range from −0.75988e to −0.71221e, showing that some electron density of O and N is transferred to copper. For **2**, the net charges of O range from −0.84627e to −0.70992e and N range from −0.84469e to −0.72266e.

By comparing the atomic net charges: (1) net charges of oxygen are more negative than nitrogen. Similarly, net charges of the interval ring nitrogens are more negative than amino nitrogens; (2) net charges of the coordinated nitrogens are more negative than uncoordinated nitrogens for **1**; and (3) net charges of nitrogens in **1** are more negative than nitrogens in **2**. Similarly, net charges of oxygens in **1** are more negative than oxygens in **2**, due to MA and adipate bonded to copper in **1**, while in **2** these ligands do not bond to metal atoms.

3.5. *X-ray powder diffraction of 1*

XRD analysis was used to characterize the new products. Sharp line diffractograms were obtained in all cases, indicating good sample crystallinity. Comparison of diffraction patterns was used to confirm that the products were single-phase materials.

As is shown in figure S6, homogeneity of **1** is confirmed by XRD analyses and peaks are in good agreement with those calculated from X-ray single crystal diffraction data.

3.6. *Thermogravimetric properties*

TGA was carried out to examine the thermal stability of **1**. As shown in figure S7, the TGA curves of decomposition of **1** show two stages of thermal decomposition. The first occurs within the temperature range 78°C to 183°C with the mass loss of 3.16%, corresponding to the release of one lattice water (calculated value 3.22%). When the temperature is above 183°C, the product begins to lose ligands and the framework is decomposed. CuO is assumed to be the final residual product at 880°C with the total mass loss of 30.48% (calculated mass loss of 28.60%), which might be due to some carbonaceous residue in the final solid phase.

3.7. *Photoluminescent properties*

The fluorescence spectra of the ligands and the compounds were measured in the solid state at room temperature in order to investigate the interaction between the metal ion and the MA ligand. Upon excitation at 260 nm, MA exhibits strong luminescence ($\lambda = 352$ nm), while the compounds exhibit luminescence at 300 nm for **1** and 405 nm for **2**.

Comparison of the photoluminescent data shows that: (1) the fluorescent intensity of free MA is stronger than the compounds containing MA due to abundant hydrogen bonding interactions delocalizing electronic density in the ring of MA and (2) there is a blue shift in **1** and a red shift **2** with fluorescence intensity of **1** weaker than **2**, probably because paramagnetic Cu(II) of **1** can weaken ligand-based luminescence [42].

4. Conclusions

Hydrothermal synthesis, crystal structures, and properties of the first metal–MA–adipate binuclear copper complex and a supramolecular architecture, $[Cu_2(MA)(ad)_2] \cdot H_2O$ (**1**) and $(MA) \cdot (H_2ad) \cdot H_2O$ (**2**) (MA = melamine; H_2ad = adipic acid), have been accomplished. Complex **1** exhibits an interesting noninterpenetrated pseudo-pcu metal–organic 3-D architecture constructed from a four-connected SBU. MA has strong coordination ability to copper, easily forming a 3-D metal–organic supramolecular framework.

Supplementary material

Tables of atomic coordinates, isotropic thermal parameters, complete bond distances, and angles have been deposited with the Cambridge Crystallographic Data Center. Copies of this information may be obtained free of charge by quoting the publication citation and deposition numbers CCDC: 723378 for **1** and 723380 for **2**, from the Director, CCDC, 12 Union Road, Cambridge, CB2 1EZ, UK (Fax: +44–1223–336033;

Email: deposit@ccdc.cam.ac.uk or www: http://www.ccdc.cam.ac.uk). Supplementary material associated with this article can be found free of charge in the online version.

Acknowledgements

We wish to express our sincere thanks to National Natural Science Foundation of China (No. 20771051) and Education Foundation of Liaoning Province (Grant No. 2007T093) for financial assistance.

References

[1] M. Eddaoudi, J. Kim, N. Rosi, D. Vodak, J. Wachter, M. O'Keeffe, O.M. Yaghi. *Science*, **295**, 469 (2002).
[2] D.F. Sun, R. Cao, Y.C. Liang, Q. Shi, W.P. Su, M.C. Hong. *J. Chem. Soc., Dalton Trans.*, 2335 (2001).
[3] J.L.C. Rowsell, O.M. Yaghi. *Microporous Mesoporous Mater.*, **73**, 3 (2004).
[4] J.S. Seo, D. Whang, H. Lee, S.I. Jun, J. Oh, Y.J. Jeon, K. Kim. *Nature*, **404**, 982 (2000).
[5] H.B. Zhu, G. Xu, J.F. Ji, S.H. Gou. *J. Coord. Chem.*, **62**, 2276 (2009).
[6] G.B. Che, C.B. Liu, L. Wang, Y.C. Cui. *J. Coord. Chem.*, **60**, 1997 (2007).
[7] M. Jiang, Y.T. Li, Z.Y. Wu, Z.W. Yin. *J. Coord. Chem.*, **62**, 380 (2009).
[8] P.P. Long, Q. Zhao, J.X. Dong, J.P. Li. *J. Coord. Chem.*, **62**, 1959 (2009).
[9] T. Kitano, Y. Sohrin, Y. Hata, H. Kawakami, T. Hori, K. Ueda. *J. Chem. Soc., Dalton Trans.*, 3564 (2001).
[10] J.L. Yi, Z.Y. Fu, S.J. Liao. *J. Coord. Chem.*, **62**, 2290 (2007).
[11] A. Cukurovali, I. Yilmaz, H. Özmen, M. Ahmedzade. *Trans. Met. Chem.*, **27**, 171 (2002).
[12] A. Ranganathan, V.R. Pedireddi, C.N.R. Rao. *J. Am. Chem. Soc.*, **121**, 1752 (1999).
[13] J.P. Mathias, E.E. Simanek, J.A. Zerkowski, C.T. Seto, G.M. Whitesides. *J. Am. Chem. Soc.*, **116**, 4316 (1994).
[14] J.A. Zerkowski, J.C. MacDonald, C.T. Seto, D.A. Wierda, G.M. Whitesides. *J. Am. Chem. Soc.*, **116**, 2382 (1994).
[15] J.P. Mathias, C.T. Seto, E.E. Simanek, G.M. Whitesides. *J. Am. Chem. Soc.*, **116**, 1725 (1994).
[16] M.M. Chowdhry, D.M.P. Mingos, A.J.P. White, D.J. Williams. *Chem. Commun.*, 899 (1996).
[17] E.W. Hughes. *J. Am. Chem. Soc.*, **63**, 1737 (1941).
[18] R. Dorta, H. Stoeckli-Evans, U. Bodensieck, G. Süss-Fink. *J. Organomet. Chem.*, **553**, 307 (1998).
[19] D.M.L. Goodgame, I. Hussain, A.J.P. White, D.J. Williams. *J. Chem. Soc., Dalton Trans.*, 2899 (1999).
[20] K. Sivashankar, A. Ranganathan, V.R. Pedireddi, C.N.R. Rao. *J. Mol. Struct.*, **559**, 41 (2001).
[21] J. Zhang, Z.J. Li, Y.H. Wen, Y. Kang, J.K. Cheng, Y.G. Yao. *J. Mol. Struct.*, **697**, 185 (2004).
[22] Y.Q. Yu, C.Z. Lu, X. He, S.M. Chen, Q.Z. Zhang, L.J. Chen, W.B. Yang. *J. Chem. Crystallogr.*, **34**, 905 (2004).
[23] X.L. Zhang, B.H. Ye, X.M. Chen. *Cryst. Growth Des.*, **5**, 1609 (2005).
[24] X.L. Zhang, X.M. Chen. *Cryst. Growth Des.*, **5**, 617 (2005).
[25] C. Chen, C.W. Yeh, J.D. Chen. *Polyhedron*, **25**, 1307 (2006).
[26] A.B. Wiles, D. Bozzuto, C.L. Cahill, R.D. Pike. *Polyhedron*, **25**, 776 (2006).
[27] L. Zhang, J. Zhang, Z.J. Li, J.K. Cheng, P.X. Yin, Y.G. Yao. *Inorg. Chem.*, **46**, 5838 (2007).
[28] L. Zhang, W. Li, J. Zhang, Z.J. Li, Y.Y. Qin, J.K. Cheng, Y.G. Yao. *Inorg. Chem. Commun.*, **11**, 279 (2008).
[29] L.F. Xu, X.L. Chen, H.M. Hu, B.C. Wang. *J. Mol. Struct.*, **892**, 163 (2008).
[30] A. Huczynski, J. Janczak, B. Brzezinski. *J. Mol. Struct.*, **922**, 77 (2009).
[31] G.J. Perpétuo, J. Janczak. *J. Mol. Struct.*, **891**, 429 (2008).
[32] M. Murugesu, P. King, R. Clerac, C.E. Anson, A.K. Powell. *Chem. Commun.*, 740 (2004).
[33] E.K. Brechin, E.C. Sanudo, W. Wernsdorfer, C. Boskovic, J. Yoo, D.N. Hendrickson, A. Yamaguchi, H. Ishimoto, T.E. Concolino, A.L. Rheingold, G. Christou. *Inorg. Chem.*, **44**, 502 (2005).
[34] C. Policar, F. Lambert, M. Cesario, I. Morgenstern-Badarau. *Eur. J. Inorg. Chem.*, 2201 (1999).
[35] E. Colacio, J.M. Dominguez-Vera, M. Ghazi, R. Kivekas, M. Klinga, J.M. Moreno. *Eur. J. Inorg. Chem.*, 441 (1999).

[36] G.M. Sheldrick. *SADABS, Program for Empirical Absorption Correction for Area Detector Data*, University of Göttingen, Göttingen, Germany (1996).

[37] G.M. Sheldrick. *SHELXS-97, Program for Crystal Structure Refinement*, University of Göttingen, Göttingen, Germany (1997).

[38] A.W. Addison, T.N. Rao, J. Reedijik, J. van Rijn, C.G. Verscoor. *J. Chem. Soc., Dalton Trans.*, 1349 (1984).

[39] P.K. Chattaraj, D.R. Roy, M. Elango, V. Subramanian. *J. Phys. Chem. A*, **109**, 9590 (2005).

[40] J. Aihara. *J. Phys. Chem. A*, **103**, 7487 (1999).

[41] M. Yoshida, J. Aihara. *Phys. Chem. Chem. Phys.*, **1**, 227 (1999).

[42] M.D. Allendorf, C.A. Bauer, R.K. Bhakta, R.J.T. Houk. *Chem. Soc. Rev.*, **38**, 1330 (2009).